ORIGINAL PAPER

Synthesis and properties of Co–Pt alloy silica core-shell particles

Y. Kobayashi · H. Kakinuma · D. Nagao · Y. Ando ·
T. Miyazaki · M. Konno

Abstract This paper describes a method for fabrication of
silica-coated Co–Pt alloy nanoparticles in a liquid phase process. The Co–Pt nanoparticles were prepared from $CoCl_2$
(4.2×10^{-5} M), H_2PtCl_6 (1.8×10^{-5} M), citric acid (4×10^{-4} M) and $NaBH_4$ (1.2×10^{-2} M) with a Co:Pt mole ratio
of 7:3. The silica coating was performed in water/ethanol
solution with a silane coupling agent, 3-aminopropyltrimethoxysilane (8×10^{-5} M), and a silica source, tetraethoxyorthosilicate (7.2×10^{-4} M) in the presence of the Co–Pt
nanoparticles. Observations with a transmittance electron
microscope and a scanning transmission electron microscope
revealed that the Co-rich and Pt-rich nanoparticles were coated
with silica. According to X-ray diffraction measurements, core
particles were crystallized to metallic Co crystallites and fcc
Co–Pt alloy crystallites with annealing in air at 300–500 °C.
Magnetic properties of the silica-coated particles were
strongly dependent on annealing temperature. Maximum
values of 11.4 emu/g-sample for saturation magnetization and
365 Oe for coercive field were obtained for the particles
annealed at 300 and 500 °C, respectively. Annealing at a
temperature as high as 700 °C destroyed the coating structures
because of crystallization of silica shell, resulting in reduction
in saturation magnetization and coercive field.

Y. Kobayashi · H. Kakinuma · D. Nagao · M. Konno (✉)
Department of Chemical Engineering, Graduate School of
Engineering, Tohoku University, 6-6-07 Aoba, Aramaki-aza,
Aoba-ku, Sendai 980-8579, Japan
e-mail: konno@mickey.che.tohoku.ac.jp

H. Kakinuma
e-mail: kakinuma@mickey.che.tohoku.ac.jp

D. Nagao
e-mail: nagao@mickey.che.tohoku.ac.jp

Present Address:
Y. Kobayashi
Department of Biomolecular Functional Engineering, College of
Engineering, Ibaraki University, 4-12-1 Naka-narusawa-cho,
Hitachi, Ibaraki 316-8511, Japan
e-mail: ykoba@mx.ibaraki.ac.jp

Y. Ando · T. Miyazaki
Department of Applied Physics, Graduate School of
Engineering, Tohoku University, 07 Aoba, Aramaki-aza,
Aoba-ku, Sendai 980-8579, Japan
e-mail: ando@mlab.apph.tohoku.ac.jp

T. Miyazaki
e-mail: miyazaki@mlab.apph.tohoku.ac.jp

1 Introduction

Magnetic nanoparticles can be used as various high technology materials such as ferrofluids [1], microwave
absorbers [2], biomedical and medical treatments and
analyses [3], and magnetic storage media [4, 5], etc.
Magnetic nanoparticles of metal oxides such as ferrites
have been the most extensively studied among various
magnetic materials [6–12]. A study on magnetic nanoparticles of pure metals such as Fe, Co and Ni has also been
carried out [13–19]. The pure metals have good magnetic
properties, and their nanoparticles are, however, easily
oxidized in air, which spoil their magnetic properties. On
the other hand, metal alloy composed of the magnetic
metals is chemically stable [20]. Other characteristics of
the magnetic metal alloy are magnetically anisotropic
properties [21], and the properties are suitable for magneto
optical storage media [22–26]. Co–Pt alloy is a candidate

for high-density magnetic recording media, because the Co–Pt alloy exhibits high magnetic anisotropy and good chemical stability to oxidation [27–31].

Various methods for the synthesis and characterization of Co–Pt alloy nanoparticles have been reported. According to Park et al. [32], Co–Pt nanoparticles can be fabricated with injection of hot platinum hexafluoroacetilacetonate/oleic acid/toluene solution into cobalt carbonyl/toluene solution. The method for producing the Co–Pt nanoparticles could be extended to preparation of Co–Pt core-shell particles. Yu et al. synthesized Co–Pt nanoparticles with sizes of 2–5 nm with reduction of Co^{2+} and Pt^{4+} by $NaBH_4$ in reverse micelles composed of water, AOT and isooctane [33]. Almost unity atomic ratio of Co to Pt provided the highest coercive field. Shevchenko et al. [34] prepared $CoPt_3$ nanoparticles by reduction of platinum acetylacetonate and thermal decomposition of cobalt carbonyl in the presence of 1-adamantanecarboxylic acid in a high-boiling coordinating solvent mixture (hexadecylamine/diphenyl ether), in which 1-adamantanecarboxylic acid and hexadecylamine acted as stabilizing agents. The particle size could be tuned from 3 to 18 nm with their method. Sobal et al. reported that Pt–Co core-shell nanoparticles with a core size of 2.6 and a shell thickness of 2.5 nm were synthesized with a two-stage route, which involved thermal decomposition of cobalt carbonyl in the presence of Pt nanoparticles in diphenyl ether containing oleic acid and oleylamine [35]. Organic compounds such as carbonyl, toluene, isooctane, etc. were used, though these methods could produce CoPt composite nanoparticles well. However, the use of such organic compounds is harmful and hazardous. Gibot et al. proposed an aqueous route for preparing CoPt nanoparticles, in which an aqueous solution of hydrazine was added to an aqueous solution containing H_2PtCl_6, $(CH_3COO)_2Co$ and surfactant [36]. Du et al. prepared CoPt nanoparticles in ethanol with a two-stage route with the use of $NaBH_4$ as a reducing agent and PVP as a surfactant [37].

In general, nanoparticles show a tendency to aggregate forming larger entities. Therefore, the magnetic particles must be separated to preserve magnetic properties that each magnetic particle acting as a single magnetic dipole reveals. Coating of the magnetic nanoparticles with silica shell, which has been employed by several authors [38–44], is a candidate for preventing the formation of aggregation. The coating also stabilizes particles chemically and enables surface-modification that allows the preparation of non-aqueous colloids and control of interparticle interactions.

We developed [45] a technique for silica coating of Co nanoparticles prepared from aqueous solutions of inorganic salts. Co ions were reduced with $NaBH_4$ in the presence of citric acid stabilizer to generate Co metallic nanoparticles, which were silica-coated by a sol-gel method after surface modification with a silane-coupling agent. In a preliminary

work previously reported, the technique was extended to silica coating of CoPt alloy nanoparticles, which were prepared with simultaneous reduction of ions of Co^{2+} and Pt^{4+} by $NaBH_4$ [46]. Since Yu et al. verified that composition atomic ratio of Co to Pt at around unity gave the highest coercivity [33], CoPt alloy nanoparticles were prepared at equal concentrations of Co^{2+} and Pt^{4+} to adjust atomic ratio of Co to Pt to unity in the previous work. However, according to XRD measurements, atomic ratio of Co to Pt in the silica-coated Co–Pt particles was lower than unity, though mechanism for the difference between the atomic ratios obtained from initial concentrations and the XRD measurements is still unclear. In a present paper, silica-coated CoPt nanoparticles were prepared at initial atomic ratio of Co higher than unity to increase atomic ratio of Co in the silica-coated particles. More precise characterization was also performed for understanding of silica-coating mechanism, which would be required to find out reaction conditions that produce magnetic particles suitable for practical use. Their magnetic properties were also studied in the present work.

2 Experimental

Cobalt chloride hexahydrate ($CoCl_2 \cdot 6H_2O$) (Wako Pure Chem. Ind., 99.5%) and hydrogen hexachloroplatinate (IV) hexahydrate ($H_2PtCl_6 \cdot 6H_2O$) (Wako Pure Chem. Ind., 98.5%) were used as cobalt and platinum precursors, respectively. Sodium borohydride (Wako Pure Chem. Ind., 90%) and citric acid monohydrate (Wako Pure Chem. Ind., 99.5%) were used as reducing and stabilizing reagents for preparation of Co–Pt nanoparticles, respectively. Special grade reagents of 3-aminopropyl-trimethoxysilane (APS) (Aldrich, 97%), tetraethylorthosilicate (TEOS) (Wako Pure Chem. Ind., 95%) and ethanol (Wako Pure Chem. Ind., 99.5%) were used for silica coating. All the chemicals were used as received. Ultrapure deionized water (resistivity higher than 18 MΩ·cm) was used in all the preparations.

Preparation of Co–Pt particles was performed with a method similar to the previous paper [44]. Concentrations of Co^{2+} and Pt^{4+} were equal to adjust atomic ratio of Co to Pt to unity in the previous work. However, an atomic ratio of Co:(Co + Pt) in the silica-coated particles was below 0.08 (Co:Pt = 0.08:0.92). In the present work, to increase Co ratio, an atomic ratio of Co:Pt was adjusted to not unity but 7:3. Aqueous solutions of 0.8 M $CoCl_2$ (52.5 μL) and 0.4 M H_2PtCl_6 (45 μL) were simultaneously added to 200 mL of 1.2×10^{-2} M $NaBH_4$ in a deaerated aqueous solution containing citric acid (4.0×10^{-4} M), and particle formation gave rise to a gray coloration of the solution. Nitrogen bubbling was maintained during the reactions. Silica coating was performed by addition of 800 ml of

ethanolic solution containing 14.4 μL of APS and 169 μL of TEOS (in which a molar ratio of APS to TEOS was 1:9) to 200 mL of the aqueous Co–Pt colloid, 1 min after mixing the $CoCl_2$–H_2PtCl_6 and $NaBH_4$ solutions. In the water/ethanol mixture, adsorption of APS onto the surface of Co–Pt particles should take place, followed by hydrolysis/condensation of both APS and TEOS, which results in the formation of the silica shells. For crystallization, the silica-coated Co–Pt particles were separated from the solution with centrifugation, dried and annealed in air at temperatures between 200 and 700 °C for 2 h.

The samples were characterized with transmission electron microscopy (TEM), scanning transmission electron microscopy (STEM), X-ray diffraction (XRD), thermal analysis and vibrating sample magnetometry (VSM). A Zeiss LEO 912 OMEGA microscope was used for TEM at 100 kV of accelerating voltage. A Hitachi High-Technologies HD-2000 microscope equipped with an energy dispersive X-ray fluorescence spectrometer (EDX) was used for STEM at 200 kV of operating voltage. Samples for TEM and STEM were prepared by dropping and evaporating the obtained particle colloid on top of a collodion-coated copper grid. XRD measurements were made with a Rigaku RU-200A diffractometer at 40 kV and 30 mA with CuKα radiation. A thermal analysis (SII SSC5200 TA station TG/DTA220) was applied to the particles in flowing air at a heating rate of 10 °C/min. VSM measurements of silica-coated Co–Pt powder were made at room temperature with a Toei VSM-5–15 magnetometer.

3 Results and discussion

3.1 Structure of silica-coated Co–Pt particles

Figure 1 shows TEM images of silica-coated Co–Pt particles as-prepared and annealed at various temperatures. Darker and lighter parts of particles were Co–Pt and silica, respectively. Multiple cores were observed in the as-prepared silica-coated particles formed. For annealing temperatures of 300 and 500 °C, the cores were clearly differentiated from the shell. At a temperature as high as 700 °C, sintering took place among the particles, and no core-shell structure was observed. In the previous work

Fig. 1 TEM images of silica-coated Co–Pt particles as-prepared (**a**) and annealed at 300 (**b**), 500 (**c**) and 700 °C (**d**)
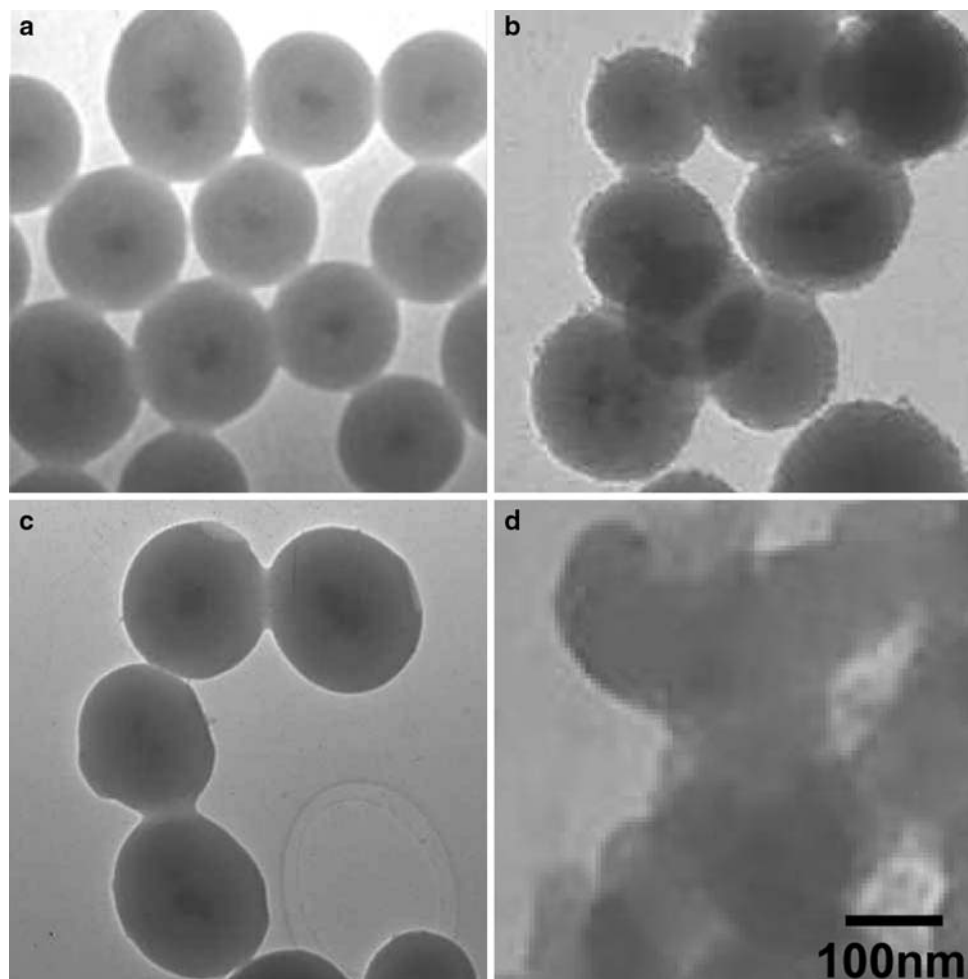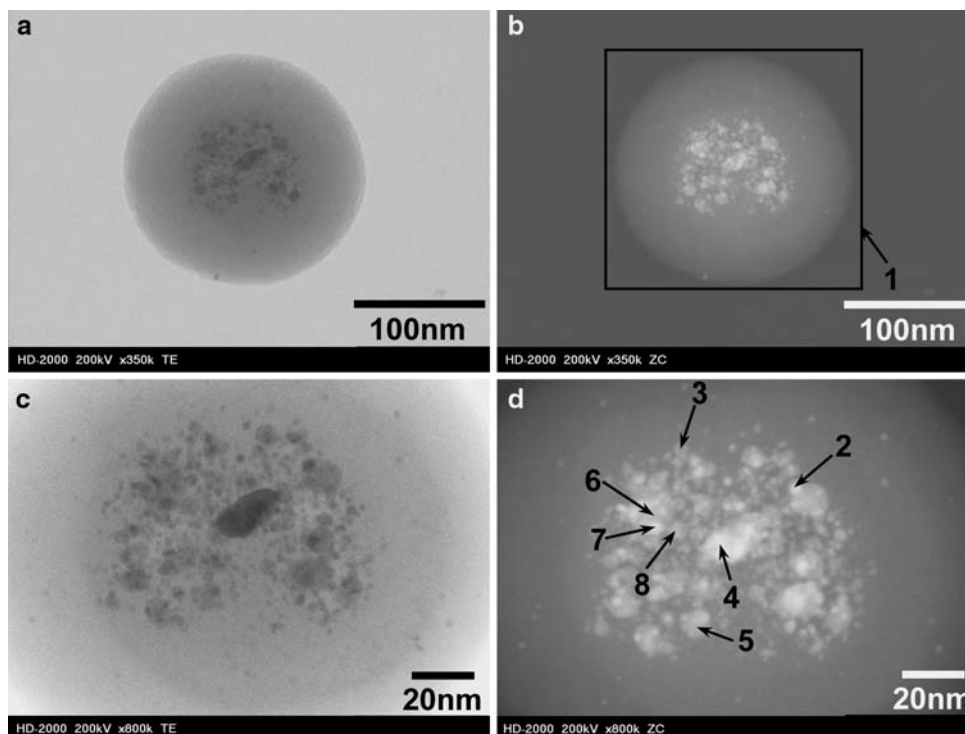
Fig. 2 STEM images of silica-coated Co–Pt particles annealed at 500 °C. Images (**a**) and (**c**) were taken in a bright field, and (**b**) and (**d**) are dark-field images for (**a**) and (**c**), respectively. High magnification images for (**a**) and (**b**) are shown in (**c**) and (**d**), respectively. Arrows with numbers 1–8 stand for points analyzed with EDX

concerning silica-coated Co–Pt particles [46], annealing at a temperature as high as 600 °C led to spread of a slightly darker area, which implied that cobalt diffused toward the silica shell. Probably, similar tendency was also observed in the present work.

Precise observation of the silica-coated particles was performed with STEM. Figure 2 shows STEM light-field and dark-field images of silica-coated Co–Pt particles annealed at 500 °C. The core was composed of a number of nanometer-sized particles. Most particles were slightly separated. Table 1 shows results of the EDX analysis that were performed for points shown with arrows in the dark-field images (Fig. 2b, d). Whole area of the particle (an arrow 1) had Co and Pt ratios of 84.5 and 15.5 atom%,

Table 1 EDX analysis results of silica-coated Co–Pt particles. Analysis points 1–8 were indicated with arrows in the dark-field images of the Fig. 4

Point	Co (atom%)	Pt (atom%)
1	84.5	15.5
2	30.7	69.3
3	19.0	81.0
4	81.8	18.2
5	29.6	70.4
6	88.8	11.2
7	62.0	38.0
8	31.7	68.3

respectively, which roughly reflected the initial Co:Pt ratios of 7:3. Particles in the core were generally classified into two groups; Co-rich (arrows 4, 6, 7) and Pt-rich (arrows 2, 3, 5, 8). This result implied that Co nanoparticles and Pt nanoparticles were independently produced at initial reaction stage, and then formation of Co–Pt alloy took place. As a consequence, Co–Pt core particles did not have uniform compositions.

Figure 3 shows XRD patterns of silica-coated Co–Pt particles as-prepared and annealed at various temperatures. The XRD pattern of as-prepared silica-coated Co–Pt particles showed several peaks at 39.79, 46.51 and 68.01 degree, which corresponded to d-values of 0.2263, 0.1950, and 0.1377 nm, respectively. These d-values were between those of Pt (0.2265 (111), 0.1962 (200) and 0.1387 (220) nm) (JCPDS card No. 4–802) and fcc $CoPt_3$ (0.2224 (111), 0.1927 (200) and 0.13627 (220) nm) (JCPDS card No. 29–499), which indicated that the core particles were fcc Co–Pt alloy. These peak positions tended to shift to high angles as the annealing temperature increased.

Figure 4a shows d-values for (111) peak position versus annealing temperature. The d-value decreased with the increase in the annealing temperature. For the annealing at 300 and 500 °C, the d-values were between those of Pt and fcc $CoPt_3$. At 700 °C, the d-value was revealed between those of fcc $CoPt_3$ and fcc Co (0.2047 (111), 0.1772 (200) and 0.1253 (220) nm) (JCPDS card No. 15–806). A Co ratio of Co–Pt alloy, or an x-value of Co_xPt_{100-x}, was estimated with interpolation with the use of data in the
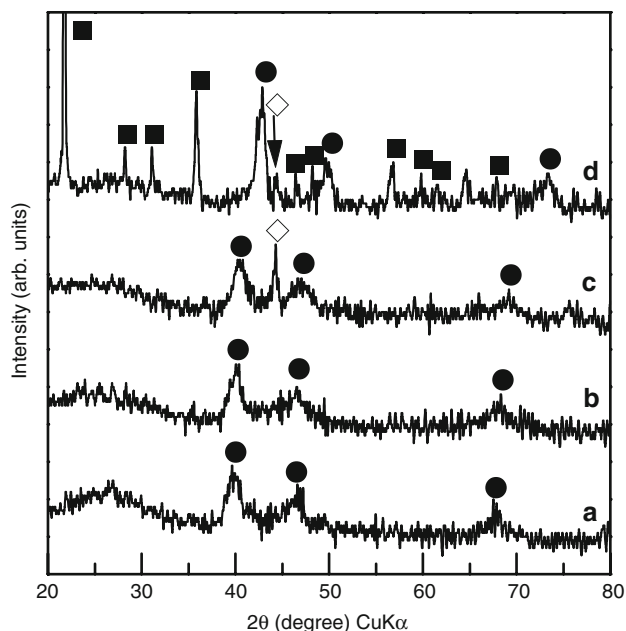
Fig. 3 XRD patterns of silica-coated Co–Pt particles as-prepared (**a**) and annealed at 300 (**b**), 500 (**c**) and 700 °C (**d**). ●: fcc Co–Pt, ■: cristobalite , ◇: fcc Co
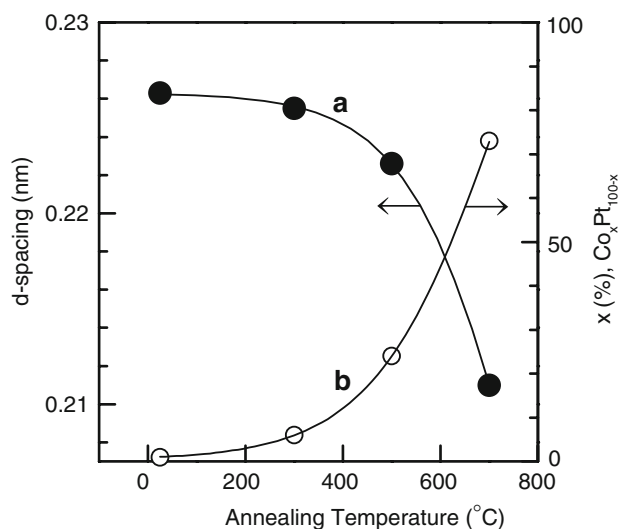

Fig. 4 d-spacing for (111) peak position (**a**) and Co ratio of Co–Pt alloy (**b**) as a function of annealing temperature

JCPDS data, as shown in Fig. 4b. In raising the annealing temperature up to 500 °C, the x-value remarkably increased to 24 (Fig. 4b), and a new peak due to fcc Co appeared at 44.30 degree besides Co–Pt peaks (Fig. 3c). These results indicated that metallic Co in the as-prepared silica-coated Co–Pt particles particles was amorphous or too small to be detected with XRD, and that the formation of Co–Pt alloy took place through crystallization of metallic Co with annealing. Consequently, the crystallization increased the x-value. According to the EDX results,

Co-rich and Pt-rich phases were present in the core for the particles annealed at 500 °C, which was supported with the XRD result showing that two phases of Co–Pt alloy and metallic Co were present in the particles.

In increasing to 700 °C, the x-value attained to 73, which corresponded to the initial Co:Pt ratio of 7:3. This result indicated that annealing at temperature as high as 700 °C was required for complete formation of Co–Pt alloy. According to the TEM observation (Fig. 1d), it was speculated that cobalt diffusion took place in the particles. Possibly, the cobalt diffusion accelerated the alloy formation. For the metallic Co peak, its intensity decreased, which indicated that most of metallic Co was used for the formation of Co–Pt alloy, and consequently, the Co–Pt alloy particles with the x-value as high as 73 were produced. Besides the peaks due to Co–Pt alloy and metallic Co, a number of new peaks marked with solid squares appeared and were identified as cristobalite silica (JCPDS card No. 39–1425). Although pure silica gel is usually crystallized from amorphous state to the cristobalite phase by annealing above 1000 °C, the crystallization temperature in the presence of sodium or borate ions can be lower because of the formation of a network structure around sodium or borate, which are likely to be present from the starting chemicals. Accordingly, the formation of cristobalite silica took place as low as 700 °C in the present work. Similar results were also observed in the previous work that studied on preparation of silica-coated Co nanoparticles [44].

Figure 5 shows TG-DTA curves for the silica-coated Co–Pt particles. A large decrease in weight, which was revealed at 100 °C accompanied with an endothermic peak
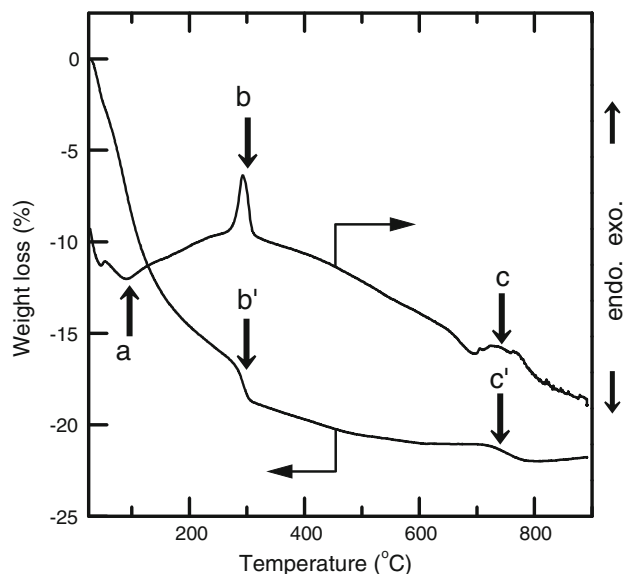

Fig. 5 TG-DTA curves for the silica-coated Co–Pt particles. See text for arrows

(an arrow a), was due to evaporation of physically adsorbed water in the particles. An exothermic weight decrease occurred at 300 °C (arrows b and b'). This weight loss was attributed to elimination with burning of citric acid. In the range of 700–800 °C, the DTA curve revealed an exothermic peak (an arrow c). This temperature range appeared to correspond to the temperature of 700 °C at which the formation of cristobalite silica was realized. This peak was accompanied with a weight loss, which was probably elimination of water from condensation of Si–OH groups. Accordingly, these results concluded that the condensation produced the cristobalite silica.

3.2 Magnetic properties

Figure 6 shows the room temperature saturation magnetization and coercive field of the silica-coated Co–Pt particles as a function of annealing temperature. The magnetization was expressed in units of emu per gram of powder. The saturation magnetization increased with an increase in the annealing temperature up to 300 °C, because of Co–Pt alloy formation provided with the annealing. A maximum value of the saturation magnetization (11.4 emu/g-sample) was obtained for the 300 °C-annealed particles. A decrease in the saturation magnetization was observed above an annealing temperature of 300 °C. This result implied that Co–Pt particles were partially oxidized with annealing in air. However, no peaks due to oxide were detected with XRD, which might mean that the oxide was too fine to be detected with XRD. The coercive field increased with an increase in the annealing temperature up to 500 °C, since formation of Co–Pt alloy was accelerated with the

annealing. A maximum value of the coercive field (365 Oe) was obtained for the 500 °C-annealed particles. A decrease in the coercive field was observed above an annealing temperature of 500 °C. The partial oxidation of Co–Pt particles might have influenced the coercive field, though its mechanism is still unclear.

4 Conclusions

Co–Pt alloy nanoparticles coated with uniform silica shells were prepared in a liquid phase process. Metal nanoparticles were prepared with addition of $NaBH_4$ to mixture of aqueous Co^{2+} and Pt^{4+} solutions, and the nanoparticles were silica-coated with sol–gel reaction of TEOS. Co nanoparticles and Pt nanoparticles were independently produced, and formation of Co–Pt alloy was provided with annealing. Measurement of magnetic properties showed that the silica-coated particles had a saturation magnetization of 11.4 emu/g-sample and a coercive field of 365 Oe.

Fig. 6 Room temperature saturation magnetization and coercive field of the silica-coated Co–Pt particles as a function of annealing temperature

References

1. Wagner J, Autenrieth T, Hempelmann R (2002) J Magn Magn Mater 252:4
2. Wu M, Zhang YD, Hui S, Xiao TD (2002) Appl Phys Lett 80:4404
3. Mehta RV, Upadhyay RV, Charles SW, Ramchand CN (1997) Biotechnol Technol 11:493
4. Zhang YD, Wang SH, Xiao DT, Budnick JI, Hines WA (2001) IEEE Trans Magn 37:2275
5. Weller D, Moser A (1999) IEEE Trans Magn 35:4423
6. Shang H, Wang J, Liu Q (2007) Mater Sci Eng A 456:130
7. Upadhyay C, Verma HC, Sathe V, Pimpale AV (2007) J Magn Magn Mater 312:271
8. Duong GV, Turtelli RS, Thuan BD, Linh DV, Hanh N, Groessinger R (2007) J Non-Cryst Solids 353:811
9. Gul IH, Abbasi AZ, Amin F, Anis-ur-Rehman M, Maqsood A (2007) J Magn Magn Mater 311:494
10. Baldi G, Bonacchi D, Innocenti C, Lorenzi G, Sangregorio C (2007) J Magn Magn Mater 311:10
11. Duong GV, Hanh N, Linh DV, Groessinger R, Weinberger P, Schafler E, Zehetbauer M (2007) J Magn Magn Mater 311:46
12. Maaz K, Mumtaz A, Hasanain SK, Ceyla A (2007) J Magn Magn Mater 308:289
13. Park S-J, Kim S, Lee S, Khim ZG, Char K, Hyeon T (2000) J Am Chem Soc 122:8581
14. Racka K, Gich M, Ślawska-Waniewska A, Roig A, Molins E (2005) J Magn Magn Mater 290–291:127
15. Osuna J, de Caro D, Amiens C, Chaudret B, Snoeck E, Respaud M, Broto J-M, Fert A (1996) J Phys Chem 100:14571
16. Giersig M, Hilgendorff M (1999) J Phys D 32:L111
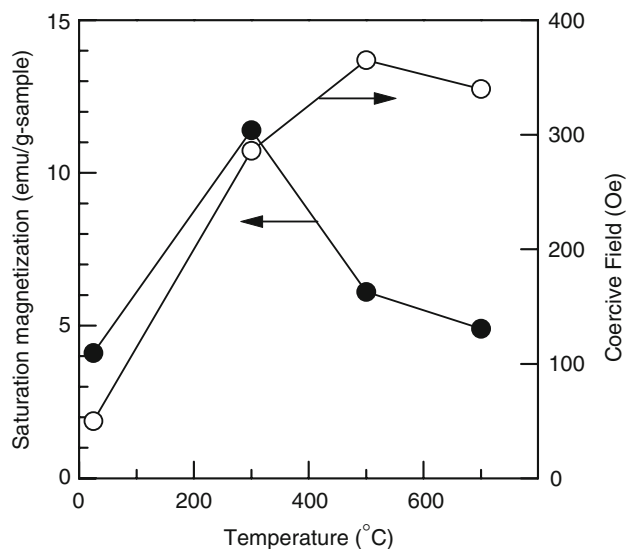17. Ely TO, Amiens C, Chaudret B, Snoeck E, Verelst M, Respaud M, Broto J-M (1999) ChemMater 11:526

18. Cordente N, Respaud M, Senocq F, Casanove M-J, Amiens C, Chaudret B (2001) Nano Lett 1:565
19. Sun Y-P, Rollins HW, Guduru R (1999) Chem Mater 11:7
20. Tyson TA, Conradson SD, Farrow RFC, Jones BA (1996) Phys Rev B 54:R3702
21. Weller D, Brändle H, Chappert C (1993) J Magn Magn Mater 121:461
22. Grange W, Maret M, Kappler J-P, Vogel J, Fontaine A, Petroff F, Krill G, Rogalev A, Coulon J, Finazzi M, Brookes N (1998) Phys Rev B 58:6298
23. Weller D, Brändle H, Gorman G, Lin C-J, Notarys H (1992) Appl Phys Lett 61:2726
24. Lin C-J, Gorman GL (1992) Appl Phys Lett 61:1600
25. Shapiro AL, Rooney PW, Tran MQ, Hellman F, Ring KM, Kavanagh KL, Rellinghaus B, Weller D (1999) Phys Rev B 60:12826
26. Chang G, Lee Y, Rhee J, Lee J, Jeong K, Whang C (2001) Phys Rev Lett 87:067208
27. Ely TO, Pan C, Amiens C, Chaudret B, Dassenoy F, Lecante P, Casanove M-J, Mosset A, Respaud M, Broto J-M (2000) J Phys Chem B 104:695
28. Carpenter EE, Seip CT, O'Connor CJ (1999) J Appl Phys 85:5184
29. Liou SH, Huang S, Klimek E, Kirby RD, Yao YD (1999) J Appl Phys 85:4334
30. Thielen M, Kirsch S, Weinforth A, Carl A, Wassermann EF (1998) IEEE Trans Magn 34:1009
31. Yamada Y, Suzuki T, Abarra EN (1998) IEEE Trans Magn 34:343
32. Park J-I, Cheon J (2001) J Am Chem Soc 123:5743
33. Yu ACC, Mizuno M, Sasaki Y, Kondo H, Hiraga K (2002) Appl Phys Lett 81:3768
34. Shevchenko EV, Talapin DV, Schnablegger H, Kornowski A, Festin Ö, Svedlindh P, Haase M, Weller H (2003) J Am Chem Soc 125:9090
35. Sobal NS, Ebels U, Möhwald H, Giersig M (2003) J Phys Chem B 107:7351
36. Gibot P, Tronc E, Chanéac C, Jolivet JP, Fiorani D, Testa AM (2005) J Magn Magn Mater 290–291:555
37. Du X, Inokuchi M, Toshima N (2006) J Magn Magn Mater 299:21
38. Ohmori M, Matijeviç E (1992) J Colloid Interface Sci 150:594
39. Ohmori M, Matijeviç E (1993) J Colloid Interface Sci 160:288
40. Philipse AP, van Bruggen MPB, Pathmamanoharan C (1994) Langmuir 10:92
41. Correa-Duarte MA, Giersig M, Kotov NA, Liz-Marzán LM (1998) Langmuir 14:6430
42. Liu Q, Xu Z, Finch JA, Egerton R (1998) Chem Mater 10:3938
43. Tago T, Hatsuta T, Miyajima K, Kishida M, Tashiro S, Wakabayashi K (2002) J Am Ceram Soc 85:2188
44. Lu Y, Yin Y, Mayers BT, Xia Y (2002) Nano Lett 1:183
45. Kobayashi Y, Horie M, Konno M, Rodríguez-González B, Liz-Marzán LM (2003) J Phys Chem B 10:7420
46. Kobayashi Y, Horie M, Nagao D, Ando Y, Miyazaki T, Konno M (2006) Mater Lett 60:2046